Appl. Phys. B 63, 229–235 (1996)

Applied Physics B Lasers and Optics

Long lifetime operation of an ArF-excimer laser

T. Saito, S. Ito, A. Tada

Opto-Electronics Research Laboratories, NEC Corporation, 1-1, Miyazaki, 4-chome, Miyamae-ku, Kawasaki, Kanagawa 216, Japan
(Fax: + 81-44/856-2224, E-mail: tsaito@oel.cl.nec.co.jp)

Received: 30 January 1996/Accepted: 18 March 1996

Abstract. An experimental investigation to improve the lifetime of a discharge-excited ArF-excimer laser is presented. The three dominant factors restricting its lifetime are CF_4 generation in the laser gas, color-center formation in the optics and input power density reduction due to electrode ablation. Copper electrodes were superior to nickel electrodes in regard to electrode ablation. A gas lifetime of more than 10^9 shots (about one month at 400 Hz) is shown for an ArF-excimer laser with a liquid-nitrogen trap and high-temperature zirconium alloy trap.

PACS: 42.55

Discharge-excited rare-gas halide excimer lasers are attractive sources of high-power, high-efficiency ultraviolet light. Because of their vacuum ultraviolet (VUV) wavelengths (193 nm), ArF-excimer lasers are promising light sources for microlithography for 1-Gbit dynamic random access memories. They are also useful for thin-film formation of high-T_c oxide super-conductors and photorefractive keratectomy. The lifetimes of ArF-excimer lasers, however, are shorter than those for XeCl- and KrF-excimer lasers [1]. This short gas lifetime of ArF-excimer lasers can be attributed to the large absorption of VUV laser light by various impurities and the high pumping power density, more than several MW/cc, for high-efficiency laser oscillations. Also, the high-intensity VUV laser pulse deteriorates optical components. Therefore, ArF-excimer lasers are mostly limited for use as laboratory tools. In this work, we elucidated the dominant factors that restrict the ArF lifetime and developed techniques for improving the lifetime.

The factors resulting in reduced laser power that are elucidated in this work are gas contamination, optics deterioration and electrode ablation. It is well known that various impurities contaminate the laser gas [2, 3]. Their impurities reduce the laser output power due to the absorption of laser light, and the quenching of the excimer or precursors. ArF-excimer laser performance is very sensitive to these impurity concentrations, compared with XeCl- and KrF-excimer lasers. It is important to select carefully the materials that constitute the laser. It was clarified that fluoroplastics generate CF_4 impurity in the vicinity of VUV laser photons [4, 5]. In our previous study, alumina ceramic insulator was used to mount the electrode assemblies inside the laser cavity instead of Teflon™. The results indicate that their gas lifetime was drastically improved. More than 10^7 shots gas lifetime was achieved without gas purification [6]. However, impurity generation cannot be prevented completely. Even a few tens of ppm (parts per million) of impurities significantly affect ArF-laser performances. Gas-purification techniques are essential to achieve much longer lifetimes.

Optics deterioration is caused by dust contamination and color-center formation, etc. The dust is generated from the electrodes and spark preionizers by the discharge. This causes transmittance reduction in the windows due to an accumulation of the dust on the surfaces of the windows attached to the laser gas. This contamination problem can be rectified by flushing the surfaces of the windows with clean gas. Tennant and Peterson [7] reported that the contamination can be decreased to one-tenth with this technique for a XeF-excimer laser. Color centers are crystal-lattice defects that absorb specific wavelengths of light [8–10]. Their formation directly reduces laser power when the absorption wavelengths overlap the laser wavelength. Color centers increase with continued exposure, reducing the transmittance capability. It is important to select high-purity materials because color-center formation depends on the purity of materials.

Influences of electrode ablation for laser performance appear after long-term operation, compared with the influences of gas contamination and mirror deterioration [6]. Electrode-profile deformation due to the ablation affects laser performance such as laser power and beam profile. Spark preionizers preionzing the discharge region from both sides of electrodes, which are used in commercial excimer lasers, cannot control the discharge width. The discharge width depends primarily on electrode profile. This differs from the X-ray preionizer,

which can control the discharge width by changing the X-ray irradiation region. Therefore, the discharge condition by the spark preionizer changes due to electrode ablation.

This paper describes and experimental investigation to improve the ArF-excimer laser lifetimes. An over 10^9 shot gas lifetime is also presented.

1 ArF-excimer laser system

The developed ArF-excimer laser is shown schematically in Fig. 1. The laser consists of a stainless steel vessel with a volume of 66 l. It has a nickel-plated surface, and is equipped with gate valves, making it possible to change the windows without refilling the laser gas. Alumina ceramic insulator is used to mount the electrode assemblies inside the laser vessel because of its high stability to withstand F_2 gas and its composition without carbon components. To remove the dust generated from electrodes and spark preionizers by discharge, a small part of the laser gas is introduced to the dust filter installed outside the laser vessel by centrifugal fans. The laser has a charge transfer circuit with automatic UV spark preionizer and magnetic assist configuration. Excitation was by means of a thyratron with switched the 26 nF storage capacitor charged below 30 kV. This laser can generate an average output power of 45 W at 400 Hz. The pulse duration is about 18 ns. The optical resonator consists of a high-reflectivity rear mirror and a 70% transmittance output coupler. These mirrors are formed from MgF_2 substrates, whose surfaces are coated with dielectric materials, and serve as pressure windows. This laser has Chang-profile electrodes 55 cm long and 3 cm wide [11]. Laser power and beam profile were measured with a disc calorimeter (38-0803, SCIENTECH INC.) and a CCD camera (TM-765E, PULNIX), respectively. To evaluate mirror deterioration, transmittance of mirrors was measured with a photo spectrometer (UV-3100, SHIMADZU).

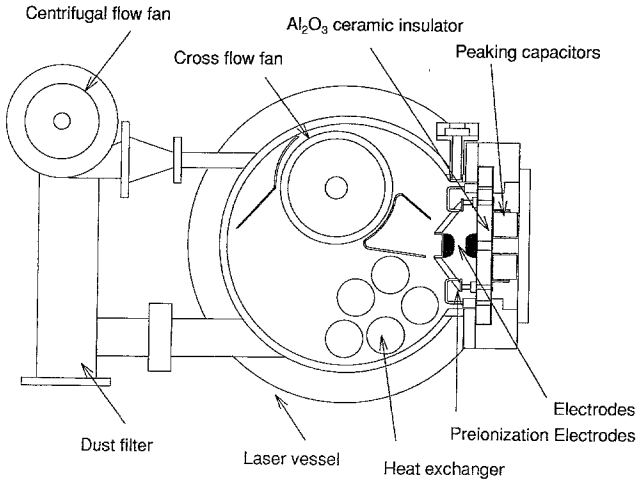

Fig. 1. Schematic cross-sectional view of the ArF-excimer laser

Figure 2 shows a schematic diagram of the system. The gas purifier, which is connected to the ArF-excimer laser, has two units [6]. One consists of a liquid-nitrogen trap and a particle filter. The condensable impurities, such as CO_2, HF, CF_2O and SiF_4, whose vapor pressures are sufficiently low at liquid-nitrogen temperature, can be effectively removed with this unit [2]. The surfaces of the laser windows are flushed with clean gas through this unit to suppress dust contamination. The other unit consists of an activated charcoal trap to remove F_2, and a high-temperature zirconium alloy trap to remove mainly air components. The activated charcoal trap is controlled at room temperature and the zirconium alloy trap is at 420 °C. The laser gas is closed-cycle recirculated between the laser and the purifier with a metal-bellows pump and a diagram pump. The laser gas diagnostic system is equipped with a Fourier-transform infrared spectrometer (FTIR-8100, SHIMAZDU), a gas chromatography mass spectrometer (GCMS-QP2000A, SHIMAZDU), an F_2 gas analyzer (CAF-100, CENTRAL GLASS), and an O_2 analyzer ($E_{COA}Z$, DAIICHI NIKKEN). These instruments were directly connected to the laser vessel.

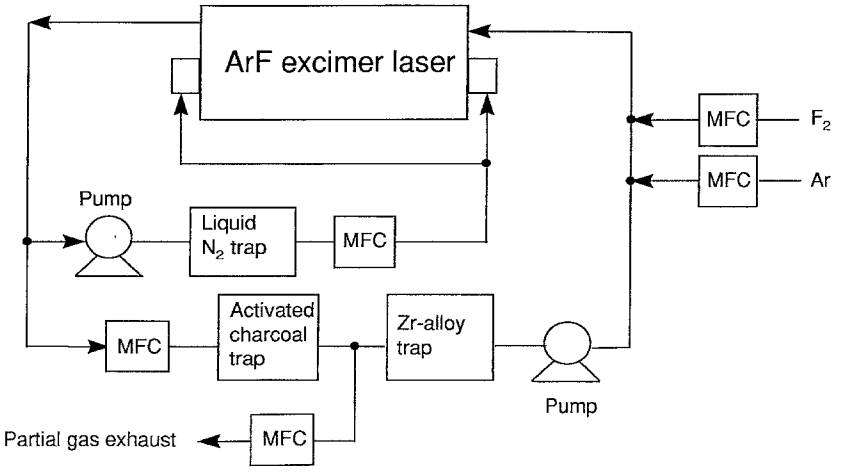

Fig. 2. Schematic diagram of the ArF-excimer laser system

2 Results and discussion

2.1 Gas contamination

The gases used for this study were F_2 (99.95% purity), Ar (99.995%) and Ne (99.999%). The laser was generally filled with 0.12% F_2, 4.6% Ar, and Ne to a total pressure of 405 kPa. The best performance was obtained with this gas mixture. Most impurities in a fresh laser gas mixture are from F_2 gas, for example, O_2, N_2, CF_4, etc. Their concentrations are all below 1 ppm. Impurities produced by the discharge in the ArF-excimer laser were identified using FTIR, GCMS and an O_2 analyzer. Figure 3 shows the infrared absorption spectrum for the laser gas after 10^7 shot operation without gas purification, measured with FTIR. The laser operated at a constant-voltage mode of 400 Hz. The F_2 concentration was kept constant by intermittent F_2 injections. The laser power dropped from 42 to 21 W for 10^7 shot operation. Only 58 ppm of CF_4 was detected. No other impurity peaks were detected in the infrared absorption spectrum. Neither O_2 nor N_2 of air components was detected in the measurements with the O_2 analyzer and GCMS. It was confirmed that the dominant impurity would only be CF_4 when the laser consists of halogen-resistant materials and is well-passivated by exposure to F_2. CF_4 was generated approximately linearly with the shot number and its generation rate was about 6 ppm per 10^6 shots. The CF_4 generation sources are thought to be O-rings, impurities in F_2 gas and electrode materials, and grease from fan bearings. In particular, perfluoro-poly-ether, used as bearing grease, has a chemical structure similar to Teflon, and evaporates into the laser gas. Grease and F_2 in the discharge region will generate CF_4 by photochemical reaction. If greaseless bearings can be easily used, contaminants generated in the laser gas will be drastically reduced. We also observed traces of the contaminants, HF, CO_2, O_2, N_2, CF_2O, and NF_3 in an insufficiently passivated laser. These sources are originated in atmospheric impurities, such as O_2, N_2, CO_2 and water vapor. We reduced generation rates of these impurities by repeating the passivation.

Figure 4 shows the gas contaminant effect on ArF output pulse energy as a function of impurity concentration. These data were measured using a fresh laser gas that added a known amounts of impurities. The 58 ppm of CF_4 reduced the laser power to 75%, as shown in Fig. 4. This result does not explain why the laser power decreased to half of its initial power for 10^7 shots operation. It was confirmed, however, it was a result of laser mirror deterioration due to dust contamination and color-center formation. We were able to determine this because the laser power recovered to 75% by replacing the mirror without exchanging the laser gas. It was confirmed that most of the impurities observed in this experiment can be reduced to below 1 ppm with the liquid-nitrogen trap. Even CF_4 can be reduced to 15 ppm, which reduces the laser power by only 6%. It was also confirmed that O_2 and N_2, which cannot be removed with the liquid-nitrogen trap, can be effectively removed with a high-temperature zirconium alloy trap.

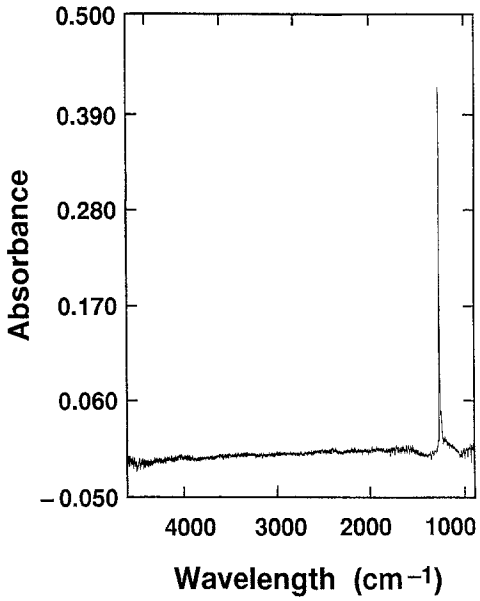

Fig. 3. Typical result obtained with FTIR, showing the spectrum of the laser gas contamination after 10^7 shot operation. The laser was operated at the constant-voltage mode of 400 Hz, and the initial power was 42 W

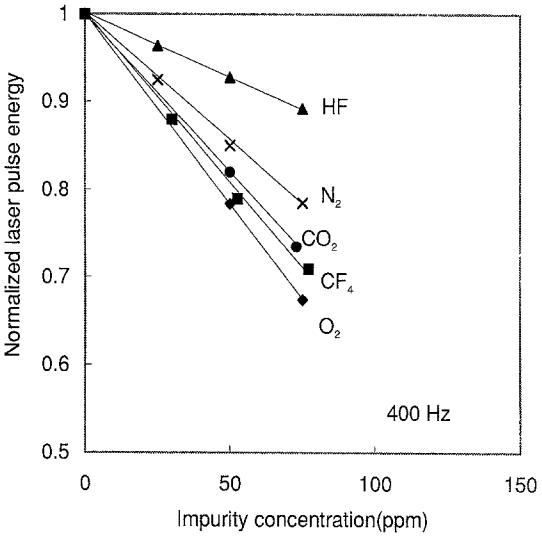

Fig. 4. Gas contaminant effects on ArF-laser output. A known amount of contaminant was introduced into a fresh gas mixture

2.2 Mirror deterioration

Mirror deterioration was caused by transmittance reduction due to dust contamination, color-center formation and reflection degradation due to deterioration of the dielectric coating. The dust contamination problem can be rectified with a clean gas flushing technique. Figure 5 shows the output coupler transmittance, before and after surface polishing, measured with the photospectrometer for various shout numbers. The average laser output

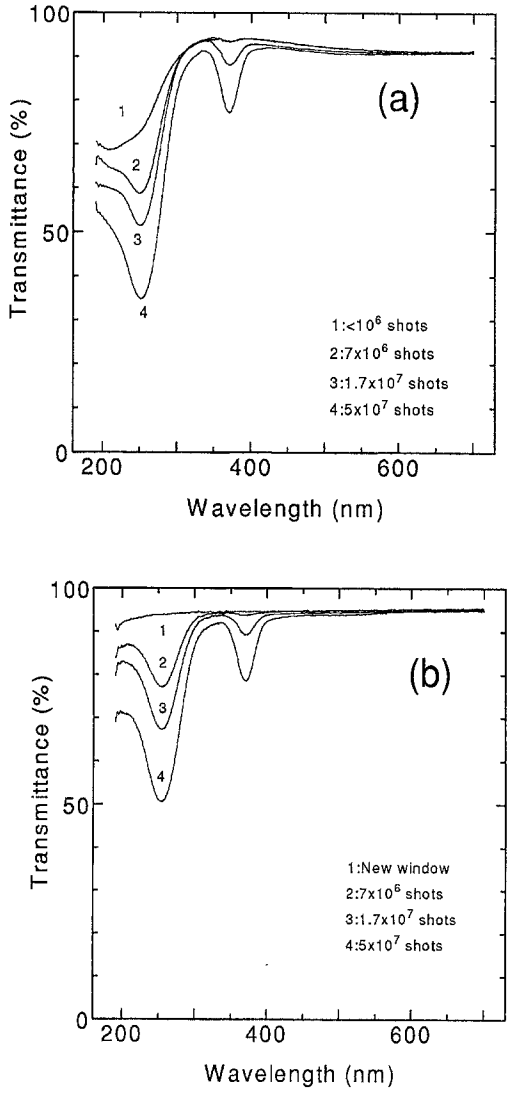

Fig. 5a, b. Transmittance for the output coupler before (**a**) and after (**b**) surface polishing, measured by photospectrometer. The average laser output power density was 23 W/cm^2 at 400 Hz

power density was 23 W/cm^2 at 400 Hz. In these experiments, the laser mirrors were flushed with the laser gas through the liquid-nitrogen trap unit. Absorption around 260 and 370 nm occurred, and they increased with shot number. These were mainly due to color centers formed in the substrates of MgF_2 mirrors. This is because the absorption did not change after surface polishing. A color center around 260 nm spread to below 193 nm, which is the ArF-laser wavelength. This color-center formation directly reduced the laser power due to the increased absorption in the laser resonator. When the absorption in ArF-laser wavelength increased to over 20%, the laser power decreased to half of the initial power in this experiment. Figure 6 shows the increased absorption coefficients of 260 nm as a function of shot number for three different MgF_2 mirrors. The impurity concentrations of these mirrors are below 10 ppm (a), 20 ppm (b) and over 100 ppm (c). Obviously, sample (a) exhibits the most hardness to ArF-laser light, because the color-center formation depends on the impurity concentration.

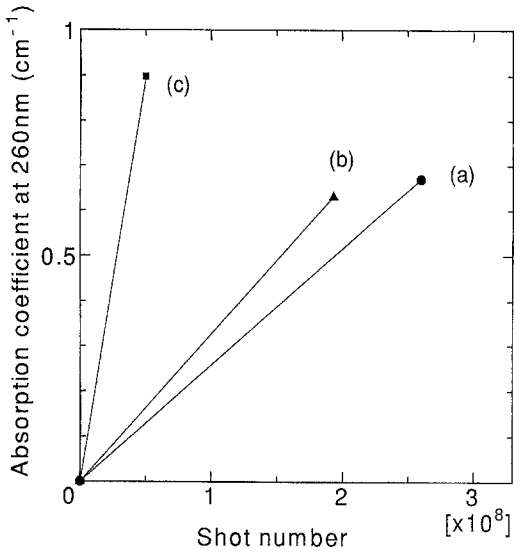

Fig. 6. Increased absorption coefficients for three MgF_2 output couplers. Impurity concentrations are below 10 ppm (a), 20 ppm (b) and over 100 ppm (c)

2.3 Electrode ablation by the discharge

Decreases in laser power due to electrode ablation were previously reported [6]. Figure 7 shows cross-sectional beam profiles before and after 1.5×10^8 shot operation. As a result of this electrode ablation, the FWHM of the beam width spread from 3.5 to 5.5 mm, and laser output power decreased to 70% with fresh laser gas and new laser mirrors. The spread of discharge width due to the electrode ablation causes the reduction of input energy density because the discharge width mainly depends on the electrode profile in the laser that the discharge region was preionized from both sides of the electrodes. As a result, the laser output power decreased due to the reduced laser gain. Figure 8 shows typical specific laser energy dependence on electrical input energy density in the tested ArF-excimer laser. Specific laser energy is approximately proportional to electrical input energy density. It was assumed that the discharge width is equal to the FWHM of the beam width. The electrical input energy density was calculated by using the measured breakdown voltage and the discharge volume. This relation between the specific laser energy and the electrical input energy density can be approximately expressed by the following equation:

$$E_{Ls} = \eta \times (E_e - E_{eth}). \quad (1)$$

Here, E_{Ls} is the specific laser energy, η is the slope efficiency. E_e is the electrical input energy density and E_{eth} is the oscillation threshold for electrical input energy density. Assuming that the discharge width (w_0) spread to $w_0 + \delta w$, and that the laser-pulse energy (E_0) reduced to E in the operation, the fraction of E/E_0 can be determined from (1), as follows:

$$E/E_0 = 1 - \delta w/w_0/(E_{e0}/E_{eth} - 1). \quad (2)$$

Here, E_{e0} is the initial input energy density. In the results shown in Fig. 7, the initial input energy density and

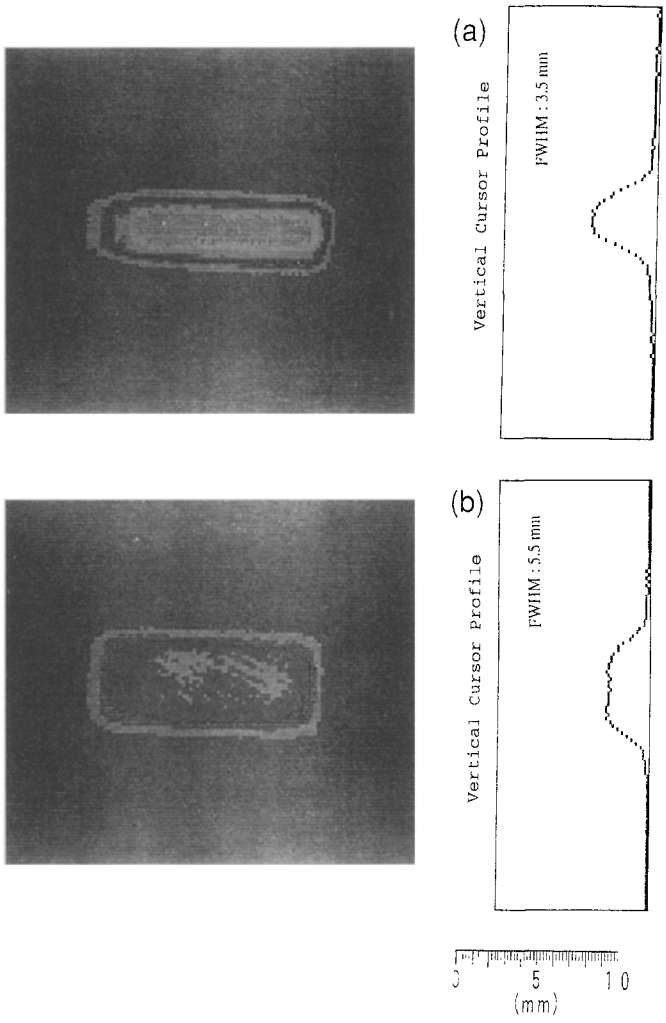

Fig. 7a,b. Beam profiles before (**a**) and after (**b**) at 1.5×10^8 shot operation. In this experiment nickel electrodes were used. The electrode spacing is 1.5 cm

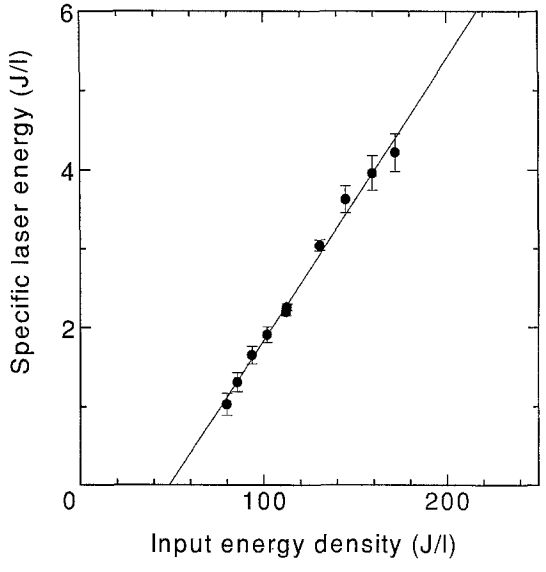

Fig. 8. Specific laser-energy dependence on input energy density

oscillation threshold were 145 and 48 J/l and the discharge width increased by 60% after 1.5×10^8 shot operation. This equation can explain the power decrease due to the electrode ablation. In addition, this equation indicates that the laser power decrease by the spread of discharge width becomes larger with decreasing initial input energy density. Higher input energy density operation may be recommended for long lifetime operation.

One reason for the electrode ablation is thought to be evaporation of electrode material by high-current constricted discharge [12]. This is affected by the discharge condition and material parameters, such as the heat conductivity and melting point. It is difficult to solve this problem because the excimer laser gas involves reactive halogen gas. We have experimentally evaluated the electrode lifetimes for three kinds of materials. Figure 9 shows normalized laser output power and cathode ablation depth as a function of shot numbers for nickel, copper and brass electrodes. For nickel and copper electrodes, the laser was operated until 1.5×10^8 shots, and for brass electrodes, the laser was operated to 1×10^8 shots. The laser was operated at 400 Hz of a constant voltage mode, and the initial input energy density was 145 J/l. Electrode spacing was 1.5 cm. It was clarified that the brass and copper electrodes have longer lifetime than nickel electrodes.

2.4 Long lifetime operation

Figure 10 shows the lifetime test results for the ArF-excimer laser system. The laser was operated at 400 Hz of

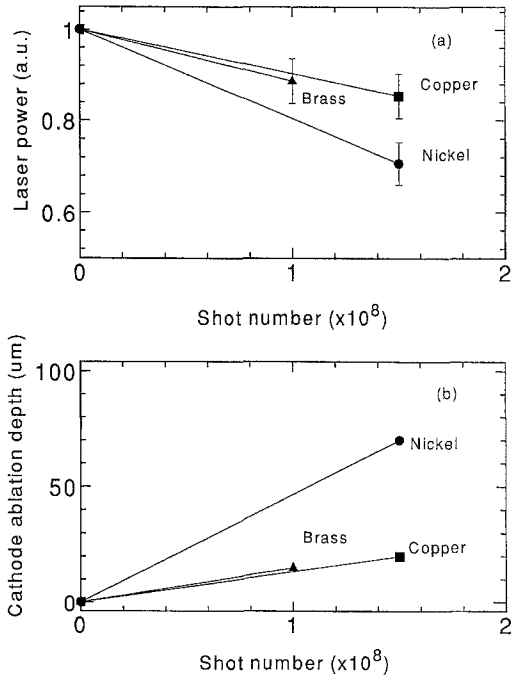

Fig. 9a, b. Laser output power and cathode ablation depth as a function of shot numbers for nickel, copper and brass electrodes. These data were measured using fresh laser gas and new laser mirrors

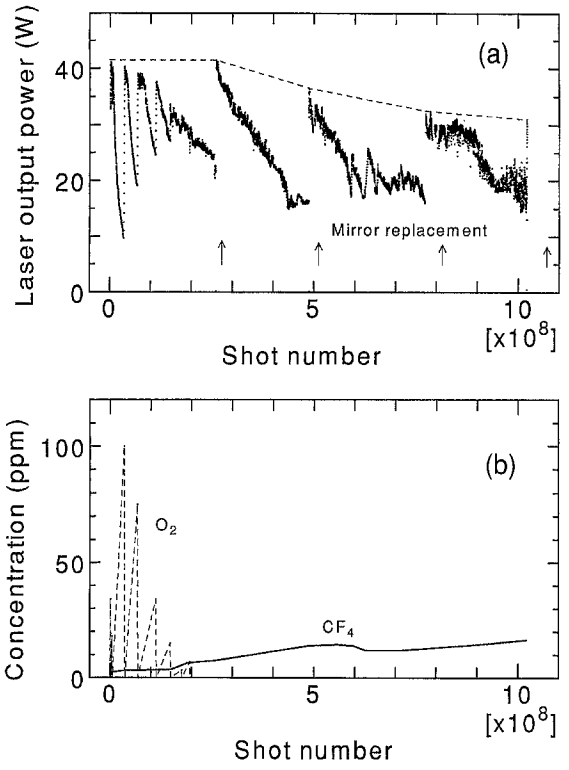

Fig. 10a, b. Laser output power (**a**) and impurity concentration (**b**) as a function of shot number for the developed ArF-excimer laser. The laser operated at 400 Hz of a constant voltage mode. The initial laser gas consisted of F_2 0.12%, Ar 4.6% in a Ne buffer. Total gas pressure was 405 kPa

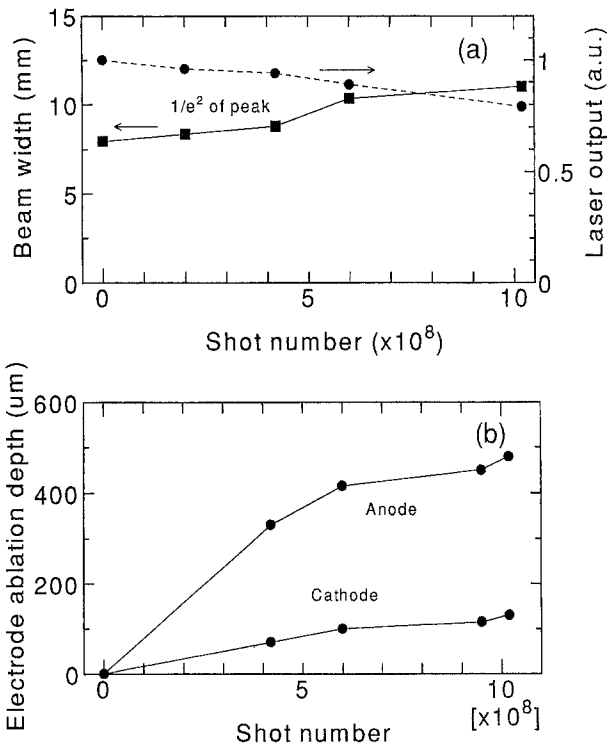

Fig. 11a, b. Laser power, beam width (**a**) and electrode ablation depth (**b**) as a function of shot number

a constant-voltage mode when the initial input energy density was 205 J/l. In this experiments, copper electrodes were used. Electrode spacing was 2 cm. The laser gas mixture was the same as in previous experiments. F_2 concentration in the laser gas was kept at 0.1–0.15% by continuous F_2 injection through a mass-flow controller. More than 90% of the maximum laser output power is obtained in this F_2 concentration. The liquid-nitrogen trap was continuously operated at 40 standard liters per minute gas flow rate. The laser mirrors were replaced four times during this test without refilling the laser gas. Deterioration of the laser mirrors was mainly due to the color-center formation. The laser power after 1×10^9 shots was 75% of initial power. This decrease was primarily due to electrode ablation. The concentration of CF_4, which was the preponderant impurity in this laser, was kept below 15 ppm with the liquid-nitrogen trap. In the initial part of this test, O_2 contaminant was generated in the laser gas mixture, which drastically reduced the laser power. This source is presumed to be water vapor adsorbing on the inner surface of the laser vessel, because this vessel was exposed to the air for the duration of one week before the test was done. As shown in Fig. 10b, O_2 can be effectively removed by intermittent operation of the high-temperature zirconium alloy trap. O_2 was not detected in the measurement after 2×10^8 shots. The volume of added gas during this test was only 1.2 times the volume of the initial laser gas. Of the added gas, 90% was Ne to dilute F_2. We confirmed that the operational cost was drastically improved in this system.

Figure 11 shows laser output power, beam width and electrode ablation depth as a function of shot number. These data, except for the one at 1×10^9 shots, were measured with other experiments. In these experiments, a fresh laser gas and new laser mirrors were used to investigate the influence of only electrode ablation. Beam width spread approximately linearly with shot number, and its increase rate was 40% of the initial one at the end of 1×10^9 shots. Laser power was reduced to 80% of the initial power due to the electrode ablation. These results coincide with the results obtained in (2). Anode and cathode ablation depths were 480 and 130 μm after 10^9 shot operation. The mass of evaporated metal from anode and cathode electrode was about 13.6 and 2.8 g, respectively. Also, the mass of evaporated metal from preionizers was measured to be 12.6 g. This value is almost in similar order to that of the main electrodes. For longer operation, it is necessary to reduce the generation of dust, because dust causes damage of fan bearings as well as window contamination and discharge instability.

3 Conclusion

We elucidated the three dominant factors that restrict ArF-excimer laser lifetime and developed techniques for extending the lifetime. CF_4 was a preponderant contaminant in a well-passivated laser. O_2, generating in an

insufficiently passivated laser, drastically reduced the laser power at high repetition rate operation and can be removed with a high-temperature zirconium alloy trap. Color-center formation was a dominant form of optics deterioration when the optics were flushed with a clean gas through the liquid-nitrogen trap. An input power density reduction due to electrode ablation significantly affected the laser power decrease. The influence of electrode ablation on three materials, nickel, copper and brass was investigated. Copper and brass electrodes were found to be superior to nickel electrodes in regard to ablation. We demonstrated the longest gas lifetime, over 10^9 shots, for the developed ArF-excimer laser with the gas purification system. Gas contamination can be rectified through a gas-purification technique, and electrode ablation can be reduced by approximately selecting materials. Therefore, to achieve much longer lifetimes of ArF-excimer lasers for industrial use, the optics lifetime will be of primary significance.

Acknowledgements. The authors would like to thank Dr. K. Hotta, Mr. M. Arai, Mr. Y. Kajiki, Mr. S. Nakamura, and Dr. H. Sekita for their valuable discussions. This work was conducted in the program: "Advanced Material-Processing and Machining System", consigned to AMMTRA from NEDO, which is carried out under ISTF funded by the Agency of Industrial Science and Technology.

References

1. J. Reid, G. Bishop, S. Hastie, B. Norris, R. Weeks, E. Williams, T. Znotins: Proc. Photo-Opt. Instrum. Eng. **1041**, 186 (1989)
2. M.C. Gower, A.J. Kearsley, C.E. Webb: IEEE J. QE-**16**, 231 (1980)
3. G.M. Jurish, W.A. Von Drasek, R.K. Brimacombe, J. Reid: Appl. Opt. **31**, 1975 (1992)
4. M. Arai, S. Ito, and K. Hotta: Tech. Dig. CLEO '91, May (1991) Paper CTha4
5. J. Fujimoto, T. Ishihara, M. Mizoguchi: In Tech. Dig. CLEO '92, May (1992) Paper CTud7
6. T. Saito, S. Ito, A. Tada, K. Hotta: Tech. Dig CLEO '93, May (1993) Paper CWJ13
7. R. Tennant, N. Peterson: Doc. LA-UR-82-2268 (Los Alamos National Laboratory, NM 1982)
8. R.T. Williams: SPIE Proc. **541**, 25 (1985)
9. I. Toepke, D. Cope: SPIE Proc. **1835**, 89 (1992)
10. R.F. Blunt, M.I. Cohen: Phys. Rev. **153**, 1031 (1967)
11. T.Y. Chang: Rev. Sci. Instrum. **44**, 405 (1973)
12. R.V. Arutyunyan, V. Yu. Baranov, V.M. Borisov, A.Yu. Vinokhodov, Yu.B. Kiryukihin: Sov. J. Quantum Electron. **15**, 639 (1985)